Food Chemistry: Molecular Sciences 2 (2021) 100027

Contents lists available at ScienceDirect

Food Chemistry: Molecular Sciences

journal homepage: www.elsevier.com/locate/fochms

Development of a new water-soluble fluorescence probe for hypochlorous acid detection in drinking water

Haoyuan Yin [a], Haijun Chi [a], Zhuye Shang [a], Ali Qaitoon [b], Jianfei Yu [a], Qingtao Meng [a,*], Zhiqiang Zhang [a], Hongmin Jia [a], Run Zhang [b,*]

[a] School of Chemical Engineering, University of Science and Technology Liaoning, Anshan 114051, China
[b] Australian Institute for Bioengineering and Nanotechnology, The University of Queensland, St. Lucia, Queensland 4072, Australia

ARTICLE INFO

Keywords:
Hypochlorous acid
Responsive probe
Fluorescence analysis
Drinking water
Sensitive and selective detection

ABSTRACT

Responsive small-molecule fluorescence probe specific for target analyte detection is an emerging technology for food safety and quality analysis. In this work, we report a new water soluble small-molecule fluorescence probe (**PG**) for the detection of hypochlorous acid (HOCl) in drinking water samples. Probe **PG** was developed by coupling of a glucosamine into 10-methyl-10H-phenothiazine fluorophore with a HOCl-responsive C = N bond. The thioether is another recognition site that can be oxidized to be sulfoxide in water. Due to the specific reactions triggered by HOCl, probe **PG**'s absorption band is blue shifted from 388 to 340 nm, and fluorescence at 488 nm is more than 55-fold enhanced. Probe **PG** features high fluorescence stability in PBS buffer with varied pH, fast response and high selectivity to HOCl. The application of the probe **PG** for HOCl detection in real-world samples is demonstrated by HOCl detection in drinking water, including tap water, purified water, and spring water samples. The recoveries of this method for HOCl detection in drinking water are in the range of 99.17–102.3%. This work thus provides a new method for HOCl detection in drinking water with high precision and accuracy.

1. Introduction

Water, accounting on average of 60% of the body weight, is an essential component of a healthy balanced diet because the body relies on it to function properly. In living organisms, water is involved in all body's chemical processes, such as digestion, nutrients absorption, waste products excretion, and body temperature regulation. Drinking fluids, particularly the drinking water, are the main source (80%) of the body water. To ensure safe and high-quality drinking water to be supplied, disinfection of drinking water by chlorine has been widely adopted in water treatment for over several hundred years (Jia et al., 2019). In water, chlorine reacts to form hypochlorous acid ($Cl_2 + H_2O \rightleftharpoons HOCl + HCl$) and hypochlorite ($HOCl \rightleftharpoons OCl^- + H^+$). HOCl and OCl^- are strong oxidants that have disinfecting ability to kill 99.9% waterborne pathogens, such as bacteria, viruses, protozoa, and helminths (Block & Rowan, 2020). Nevertheless, exposure to large amount of HOCl/OCl^- could result in several disorders, such as irritation of the oesophagus, vomiting, asthma (Del Rosso & Bhatia, 2018). The major routes of HOCl/OCl^- exposure are through drinking water (5.6–28.2 μM in most disinfected drinking-water), foods, and contact with items either bleached or disinfected with it. For rats were administered OCl^- in drinking water, an oral LD_{50} was found to be 850 mg/kg of body weight. Therefore, monitoring the HOCl level in drinking water is essential because drinking water is one of the most important substances for all living organisms' survival.

In the past few decades, a variety of conventional techniques (Wu et al., 2019a, 2019b, 2019c; Zhang et al., 2018), such as chemiluminescence (Zhu et al., 2018), colorimetric (Ren et al., 2021; Shiraishi et al., 2021), electrochemical (Ordeig et al., 2005), and chromatographic (Watanabe et al., 1998) methods have been widely used for HOCl analysis in environmental and biological samples (Kwon et al., 2021). Recent research has also demonstrated that the responsive small-molecule fluorescence probes are useful tools for the detection of HOCl in water and biological samples (Bruemmer et al., 2020). In comparison with traditional methods, fluorescence analysis using responsive probes are featured with high sensitivity and selectivity, simplicity for implementation, and good biocompatibility (Kaushik et al., 2017; Wu et al., 2019a, 2019b, 2019c; Zhang et al., 2020).

* Corresponding authors.
E-mail addresses: qtmeng@ustl.edu.cn (Q. Meng), r.zhang@uq.edu.au (R. Zhang).

https://doi.org/10.1016/j.fochms.2021.100027
Received 8 March 2021; Revised 10 May 2021; Accepted 22 May 2021
Available online 27 May 2021

The development of responsive small-molecule probes has also been an attractive research field in food quality and safety analyses (Yadav et al., 2020; Duan et al., 2021; Feng et al., 2021). As a result, several fluorescence probes have recently been engineered for HOCl detection through employing different sensing reaction mechanisms, including oxidations with oxime derivatives (Zhao et al., 2011), amines (including dibenzoylhydrazine) (Chen et al., 2010; Goswami et al., 2014; Liu et al., 2011), electron-deficit C=C bond (Chen et al., 2010; Park et al., 2013; Wu et al., 2016), *p*-methoxyphenol and palkoxyaniline (Setsukinai et al., 2003; Sun et al., 2008), and group 16 elements (such as S, Se, and Te) (Ge et al., 2020; Ikeno et al., 2019; Venkatesan & Wu, 2015). The probes were thus developed by incorporating one or two these HOCl-responsive moieties with well-established fluorophores (Gangopadhyay et al., 2018; Han et al., 2020; Li et al., 2020a, 2020b), such as fluorescein, cyanine, coumarin, naphthalimide, and metal complexes (Wu et al., 2019a, 2019b, 2019c; Zhang et al., 2018). HOCl detection was then achieved through recording the changes of fluorescence signals after the response reaction. Despite the rapid progress in the development of fluorescence probes for HOCl detection, drinking water analysis necessitates a reliable analytical probe for the detection of HOCl in pure water with rapid response, high sensitivity and selectivity.

In this work, we report a new water-soluble fluorescence probe (**PG**) for the detection of HOCl in drinking water samples. **PG** was developed by incorporating a glucosamine into 10-methyl-10H-phenothiazine fluorophore by a HOCl-responsive C=N bond (Scheme 1). The thioether in phenothiazine fluorophore is another responsive moiety for HOCl detection. The glucose-conjugated probe (**PG**) has very good water solubility, allowing for HOCl detection in aqueous solution (20 mM PBS buffer, pH 7.4). **PG** is almost non-fluorescent in PBS buffer, while the fluorescence intensity is significantly increased upon HOCl-triggered cleavage of C=N bond and oxidation of thioether within 5 s. Overall, **PG** has large Stokes shift (148 nm), excellent solubility and stability in aqueous solution, high sensitivity and selectivity, rapid fluorescence response to HOCl, allowing it to be used as a tool for the detection of HOCl in drinking water samples.

2. Experimental section

2.1. Materials

10-Methyl-10H-phenothiazine-3-carbaldehyde was synthesized by following the published method (Feng et al., 2018). 10-Methyl-10H-phenothiazine and D(+)-glucosamine hydrochloride were purchased from Aladdin reagent Co. (Shanghai, China). Triethylamine, phosphorus oxychloride, metal ions (nitrate salts), anions (sodium salts) and sodium hypochlorite (NaOCl) were obtained from Sinopharm Chemical Reagent Co., Ltd. (China). Unless otherwise stated, solvents and reagents were of analytical grade from commercial suppliers and were used without further purification.

2.2. Synthesis of probe PG

Scheme S1 illustrates the stepwise synthesis procedure of **PG**. Briefly, triethylamine (0.15 mL) was added into D(+)-Glucosamine hydrochloride (0.216 g, 1.1 mmol) in 8 mL MeOH. The mixture was refluxed for 30 min, and then 10-methyl-10H-phenothiazine-3-carbal dehyde (0.241 g, 1 mmol) in 10 mL MeOH was added into the solution. The reaction mixture was refluxed for another 3 h to form a yellow precipitate. **PG** was then obtained in 67% yield after filtration and washing thrice with cooled MeOH. ^{1}H NMR (DMSO d_6, 400 MHz) δ (*ppm*) 8.08 (s, 1H), 7.52 (d, J = 1.7 Hz, 1H), 7.24–7.15 (m, 2H), 6.99 (d, J = 7.9 Hz, 3H), 6.51 (s, 1H), 4.88 (d, J = 5.3 Hz, 1H), 4.78 (d, J = 5.6 Hz, 1H), 4.69 (t, J = 7.2 Hz, 1H), 4.51 (t, J = 5.8 Hz, 1H), 3.73 (dd, J = 9.7, 5.6 Hz, 1H), 3.53–3.46 (m, 1H), 3.42 (d, J = 5.6 Hz, 1H), 3.35 (s, 3H), 3.24 (s, J = 9.7, 5.8, 2.1 Hz, 1H), 3.16 (dd, J = 11.3, 5.3 Hz, 2H), 2.82–2.75 (m, 1H). ^{13}C NMR (DMSO d_6, 100 MHz) δ (*ppm*) 160.98, 147.46, 145.03, 131.30, 128.79, 128.36, 127.29, 126.02, 123.35, 122.68, 122.04, 115.39, 114.78, 96.06, 78.58, 77.34, 75.03, 70.81, 61.75, 35.86. ESI-MS (positive mode, m/z) calcd for $C_{20}H_{23}N_2O_5S^+$: 403.1328, [**PG** + H]$^+$: found: 403.1313. M.p.: 188.1–189.1 °C.

2.3. General procedures for spectrometric analysis

Anions and biomolecules in deionized water (20 mM) were freshly prepared. HOCl solution was prepared by diluting the commercial NaOCl solution into deionized water and diluted solution was used as the stock solution stored at 4 °C (Chen et al., 2010). The HOCl concentration was determined by UV–vis analysis using its molar extinction coefficient ($\varepsilon_{292\ nm}$ = 391 M^{-1} cm^{-1}) (Chen et al., 2010). Singlet oxygen ($^1O_2$) was produced in a Na_2MoO_4-H_2O_2 system in 0.05 m carbonate buffer of pH 10.5 (Song et al., 2005). SIN-1 was used as the donor of peroxynitrite ($ONOO^-$) (Wu et al., 2018; Yang et al., 2006). Commercial H_2O_2 (30%) solution was diluted with deionized water to prepare H_2O_2 stock solution. The concentration was measured by UV–vis using the molar absorption coefficient of H_2O_2 in water ($\varepsilon_{240\ nm}$ = 43.6 M^{-1} cm^{-1}) (Chen et al., 2017). Hydroxyl radical (**.**OH) was obtained through a Fenton reaction between ammonium sulfate and hydrogen peroxide (Wu et al., 2019a, 2019b, 2019c; Zhuang et al., 2014). For spectrometric analysis, **PG** (10 mM) in 20 mM PBS buffer (pH 7.4) was added with different concentrations of analytes (total volume 3 mL). The solution was stabilized for 5 min before fluorescence and UV–vis analyses.

2.4. HOCL detection in drinking water samples

Bottled spring water and purified water samples were obtained from local supermarket. Tap water was obtained from the laboratory without any further treatment. To demonstrate the feasibility of probe **PG** for HOCl detection in these drinking water samples, **PG** (10 μM) in above drinking water was added with different concentration of HOCl (0, 0.01, 0.05, 0.1, and 0.5 mM). The mixture was stabilized for 5 min and then the fluorescence color changes of the solution was recorded under 365 nm UV light. For quantitative detection of HOCl in drinking water samples, tap water and bottled spring water were added with HOCl, and then the HOCl-spiked water samples were analysed by using **PG** (10 μM) as a probe.

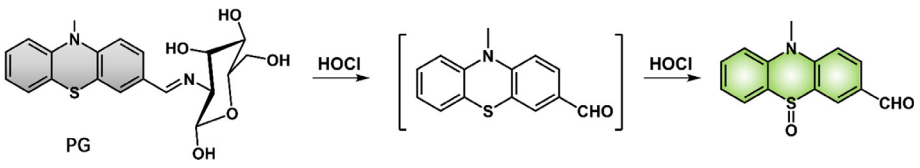

Scheme 1. Schematic illustration of the response mechanism of probe (**PG**) for HOCl detection.

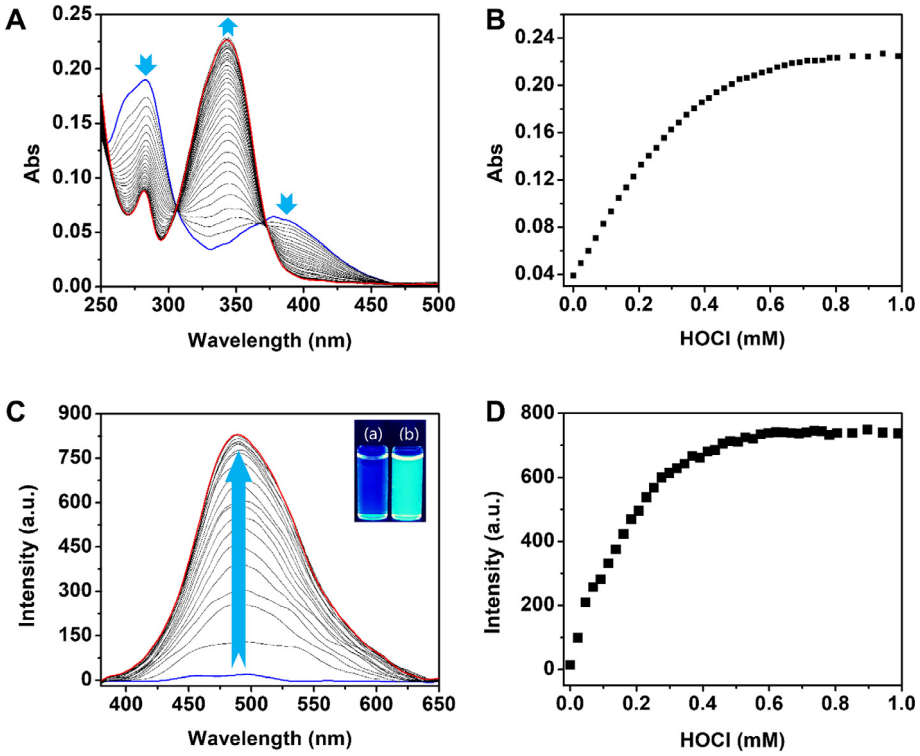

Fig. 1. UV–vis absorption and fluorescence responses of probe **PG** to HOCl in 20 mM PBS buffer of pH 7.4. (A) UV–vis absorption spectra of probe **PG** (10 μM) after reacting with increasing concentrations of HOCl (0–1 mM). (B) Absorbances of probe **PG** at 340 nm against the concentrations of HOCl. (C) Fluorescence spectra of **PG** (10 μM) after reacting with increasing concentrations of HOCl (0–1 mM). Inset: fluorescence color change of probe **PG** with (a) and without (b) HOCl. (D) Fluorescence intensities of **PG** at 488 nm against the increasing concentration of HOCl. Excitation was performed at 340 nm.

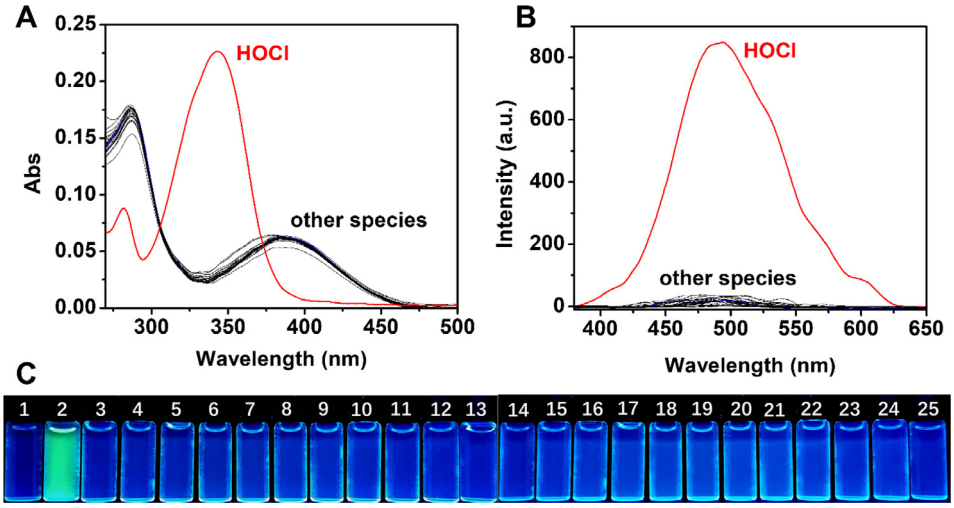

Fig. 2. UV–vis absorption and fluorescence selectivity of probe **PG** (10 μM) for HOCl detection over other interference species (0.8 mM) in 20 mM PBS buffer of pH 7.4. (A) Changes of UV–vis spectra of probe **PG** with and without various interference species and HOCl. (B) Fluorescence spectra response of probe **PG** to various interreference species and HOCl. Excitation was performed at 340 nm. (C) Fluorescence color images of **PG** in the absence and presence of various interference species and HOCl. These species include: 1. Blank, 2. HOCl, 3. Br^-, 4. AcO^-, 5. Cl^-, 6. F^-, 7. S^{2-}, 8. NO_2^-, 9. NO_3^-, 10. $^1O_2$, 11. OH^-, 12. $ONOO^-$, 13. $P_2O_7^{4-}$, 14. PO_4^{3-}, 15. HSO_3^-, 16. SO_3^{2-}, 17. SO_4^{2-}, 18. HCO_3^-, 19. HSO_4^-, 20. $H_2PO_4^-$, 21·H_2O_2, 22. **.**OH, 23. Cys, 24. Hcy, 25. GSH.

3. Results and discussion

3.1. Synthesis and characterization of probe PG for HOCl detection

The development of responsive fluorescence probes for selective and sensitive detection of various analytes in drinking water samples is contributing significantly to the food analysis (Yadav et al., 2020; Duan et al., 2021; Feng et al., 2021). In this work, we report a water soluble small-molecule probe (**PG**) for HOCl detection in drinking water samples. The probe was developed through coupling of glucosamine into 10-methyl-10H-phenothiazine fluorophore with a HOCl-responsive C=N bond. The conjugation of glucose offered **PG** good water solubility. Together with the thioether recognition moiety in phenothiazine fluorophore, probe **PG** is capable of reacting with

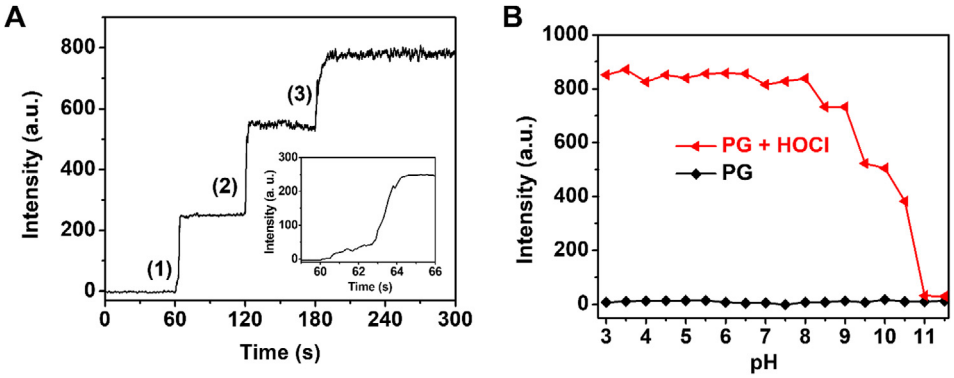

Fig. 3. Time and pH dependent fluorescence response of probe **PG** (10 μM) to HOCl. (A) Time-dependent fluorescence changes of **PG** in 20 mM PBS buffer of pH 7.4 upon the sequential addition of 0.3 mM, 0.6 mM, 1.0 mM of HOCl. (B) pH effects on the emission intensities of **PG** before and after reacting with HOCl (0.8 mM) in aqueous solution of different pH. Excitation and emission were performed at 340 and 488 nm, respectively.

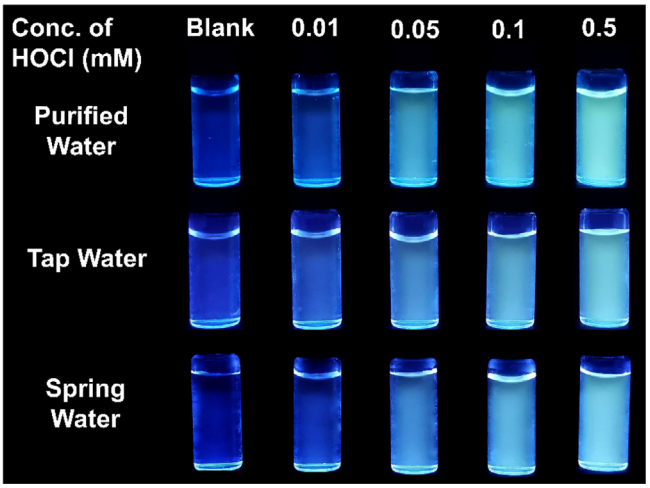

Fig. 4. Fluorescence color responses of **PG** (10 μM) in drinking water samples (purified water, tap water, and spring water) spiked with different concentrations of HOCl (0, 0.01, 0.05, 0.1, 0.5 mM) under 365 nm UV light.

HOCl to cleave the C=N bond and oxidize the thioether to sulfoxide. It has been reported that the unbridged C=N bonds containing fluorescent dyes are usually non-emissive because the C=N isomerization is the predominant decay process of excited states (Zhang et al., 2018). As a result of the HOCl-mediated C=N cleavage and formation of aldehyde and sulfoxide functionalized phenothiazine fluorophore, fluorescence of **PG** is switched on and the changes of fluorescence intensity can be recorded for HOCl detection.

As shown in Scheme S1, probe **PG** was synthesized through a two-step reaction procedure. Chemical structure of **PG** was characterized by ^{1}H NMR and ^{13}C NMR, and HRMS characterizations (Figs. S1-S3). The reaction between probe **PG** and HOCl was then examined by HRMS analyses. As shown in Fig. S4A, MS analysis (positive model) of probe **PG** showed a molecular ionic peak at m/z = 403.1313 ([**PG** + H]$^{+}$). Upon addition of HOCl, cleavage of C=N bond was observed immediately as the emergence of new peak at m/z = 242.0636 ([$C_{14}H_{12}NOS$]$^{+}$) (Fig. S4B). After 5 min reaction, oxidation reaction was observed as the emergence of another peak at m/z = 258.0588 ($C_{14}H_{12}NO_2S$)$^{+}$) (Fig. S4C). The data of HRMS analysis suggest the cleavage of C=N bond and oxidation of thioether to sulfoxide after reaction of **PG** with HOCl (Scheme 1).

3.2. UV–vis absorption and fluorescence responses of probe PG to HOCl

To investigate the UV–vis absorption and fluorescence responses of **PG** to HOCl, **PG** (10 μM) in 20 mM PBS buffer was treated with HOCl at different concentrations, and then the UV–vis absorption and fluorescence spectra were obtained after 5 min reactions. As shown in Fig. 1A, in the absence of HOCl, **PG** exhibited two intense absorption bands centred at 286 and 388 nm. Upon addition of HOCl, both absorption bands were decreased. A new absorption band (λ_{abs} = 340-nm) was emerged, and the absorbance was gradually increased with the increasing concentration of HOCl (Fig. 1B). Maximum change of the absorption spectra at 340 nm was obtained when 0.7 mM HOCl was added into the PBS solution containing **PG**.

Upon excitation at 340 nm, **PG** displayed weak fluorescence at 488 nm (Stokes shift 148 nm) in PBS buffer (20 mM, pH 7.4) with a quantum yield of 0.48%. As shown in Fig. 1C, fluorescence of **PG** at 488 nm was emerged and increased upon addition of HOCl. Green color of the **PG** solution containing HOCl was observed, indicating that the enhanced fluorescence of **PG** in the presence of HOCl can be clearly perceived even by the naked eyes. The emission intensity was over 55-fold enhanced and reached to a plateau after **PG** reacting with 0.7 mM HOCl (Fig. 1D), which is in consistent with the results of UV–vis analyses. The quantum yield was then determined to be 8.52% after **PG** reacting with HOCl.

In PBS buffer, the fluorescence stability of probe **PG** within 32 h incubation and its fluorescence response to HOCl at different time point were investigated. As shown in Fig. S5, fluorescence intensity

Table 1
Detection of HOCl in drinking water samples using **PG** (10 μM) as a probe.

Samples	HOCl level (μM)	HOCl added (μM)	HOCl found (μM)	RSD (%, n = 3)	Recovery (%)
Tap water	5.72	30	36.3	1.95	101.61
		50	56.59	2.33	101.56
		70	75.09	1.10	99.17
Spring Water	0	30	30.69	2.23	102.3
		50	49.59	2.19	99.18
		70	71.13	2.99	101.62

of **PG** in PBS buffer was not changed over 32 h incubation, while remarkable enhancement of **PG**'s emission was obtained after reacting with HOCl. Moreover, increment of fluorescence intensity of **PG** at 488 nm displayed a good linearity with the concentrations of HOCl in the range from 5 to 280 μM (R^2 = 0.995) (Fig. S6). Based on the method defined by IUPAC (3σ/k) (Mocak et al., 1997), the detection limit of **PG** for HOCl was then determined to be 1.97 μM.

Selective response of probe **PG** to HOCl was then investigated by UV–vis absorption and fluorescence spectrometric analyses. In PBS buffer of pH 7.4, **PG** (10 μM) in water was added with 0.8 mM Br^-, AcO^-, Cl^-, F^-, S^{2-}, NO_2^-, NO_3^-, $^1O_2$, OH^-, $ONOO^-$, $P_2O_7^{4-}$, PO_4^{3-}, HSO_3^-, SO_3^{2-}, SO_4^{2-}, HCO_3^-, HSO_4^-, $H_2PO_4^-$, H_2O_2, **.**OH, Cys, Hcy, and GSH, respectively. As shown in Fig. 2A, negligible changes of absorption spectra were obtained after mixing of interference species with probe **PG**. In contrast, the absorption band was clearly shifted from 388 to 340 nm upon reacting with HOCl. Selective response of **PG** to HOCl was further confirmed by fluorescence spectra analyses. As shown in Fig. 2B, fluorescence of **PG** was remarkably increased upon reacting with HOCl over other interference species. Under UV-light, green color of the **PG** solution was observed after reacting with HOCl, while no color changes were obtained upon the addition of other interference species (Fig. 2C). In addition, response of **PG** to HOCl was not affected in the presence of other interference species (Fig. S7), indicating that **PG** can specifically detect HOCl in complicated water samples.

3.3. Time and pH dependent fluorescence response of PG to HOCl

Through monitoring the emission intensity change at 488 nm with excitation at 340 nm, time dependent fluorescence response of probe **PG** to HOCl was investigated in 20 mM PBS buffer of pH 7.4. As shown in Fig. 3A, **PG** displayed weak and stable emission in buffer solution. Upon the addition of HOCl, **PG** solution showed fast response by increasing the emission intensity and the intensity reached the maximum value within 5 s (Fig. 3A inset). The emission intensity then remained at a steady level until further addition of HOCl. The results indicate that the sensing reaction of **PG** to HOCl is very fast and the produced product is fluorescence stable in PBS buffer.

Then, the pH effect on **PG**'s fluorescence response to HOCl was investigated in PBS buffer at different pH. As shown in Fig. 3B, **PG** displayed weak and stable emission in PBS buffer with pH from 3 to 11.5. Upon reacting with HOCl, remarkable enhancement in emission intensity was observed in pH 3–9. In the pH 9–10.5, response of **PG** to HOCl was gradually decreased, and in pH above 11, limited fluorescence response of **PG** to HOCl was observed. The result suggests that probe **PG** is able to detect HOCl in acidic, neutral, and weakly basic buffer solutions.

3.4. Detection of HOCl in drinking water samples

To validate the capability of probe **PG** for HOCl detection in real-world samples, **PG** was added into three kinds of drinking water samples, including bottled purified water, spring water, and tap water. Then, HOCl at different concentrations (0.01, 0.05, 0.1, and 0.5 mM) were added into the water samples. As shown in Fig. 4, under UV light, fluorescence colors of three drinking water samples were gradually changed to green with the HOCl concentration increasing from 0.01 to 0.5 mM. The enhancement of green fluorescence is attributed to the response of **PG** to HOCl in these three drinking water samples. Therefore, probe **PG** is promising to be used as a tool for the detection of HOCl by "naked eye" in drinking water samples.

The practical utility of probe **PG** for quantitative detection of HOCl in drinking water samples was further evaluated. As shown in Table 1, HOCl concentrations were found to be 5.72 and 0 μM in tap water and spring water sample, respectively. Through investigating the HOCl-spiked drinking water, the recoveries were in the range of 99.17–102.30% and the relative standard deviation (RSD) of all detections was less than 2.99%. These results clearly indicate that **PG** can be used as a tool for HOCl detection in drinking water with high precision and accuracy.

4. Conclusions

In summary, a new water-soluble responsive probe (**PG**) for HOCl detection in drinking water was developed in this work. The probe was designed by conjugating glucosamine into 10-methyl-10H-phenothiazine fluorophore with a HOCl-responsive C=N bond. The reaction of **PG** with HOCl cleaved C=N bond and oxidized the thioether in phenothiazine within 5 s. More than 55-fold enhancement in emission at 488 nm was observed, which allowed for the HOCl detection in PBS buffer. The application of this probe for the detection of HOCl in drinking water was also validated by quantification of HOCl in tap and spring water samples. The successful development of this probe thus offers a reliable tool for HOCl detection in real-world food samples.

Declaration of Competing Interest

The authors declare that they have no known competing financial interests or personal relationships that could have appeared to influence the work reported in this paper.

Acknowledgements

Financial support from the National Natural Science Foundation of China (Grants 21974016 and 21775015), the Talent Program-Outstanding Youth Science Project, Liaoning (No. XLYC1807199, Q. M.), the Scientific Research Plan Projects of Liaoning Education Department (2019LNQN03 and 2019LNJC18), Australian Research Council (DE170100092) is gratefully acknowledged.

Appendix A. Supplementary data

Supplementary data to this article can be found online at https://doi.org/10.1016/j.fochms.2021.100027.

References

Block, M. S., & Rowan, B. G. (2020). Hypochlorous acid: A review. *Journal of Oral and Maxillofacial Surgery, 78*(9), 1461–1466. https://doi.org/10.1016/j.joms.2020.06.029.

Bruemmer, K. J., Crossley, S. W. M., & Chang, C. J. (2020). Activity-based sensing: A synthetic methods approach for selective molecular imaging and beyond. *Angewandte Chemie International Edition, 59*(33), 13734–13762. https://doi.org/10.1002/anie.201909690.

Chen, S., Lu, J., Sun, C., & Ma, H. (2010). A highly specific ferrocene-based fluorescent probe for hypochlorous acid and its application to cell imaging. *Analyst, 135*(3), 577–582. https://doi.org/10.1039/B921187J.

Chen, Y., Shi, X., Lu, Z., Wang, X., & Wang, Z. (2017). A fluorescent probe for hydrogen peroxide in vivo based on the modulation of intramolecular charge transfer. *Analytical Chemistry, 89*(10), 5278–5284. https://doi.org/10.1021/acs.analchem.6b04810.

Del Rosso, J. Q., & Bhatia, N. (2018). Status report on topical hypochlorous acid: Clinical relevance of specific formulations, potential modes of action, and study outcomes. *The Journal of Clinical and Aesthetic Dermatology, 11*(11), 36–39 https://pubmed.ncbi.nlm.nih.gov/30588272.

Duan, N., Wang, H., Li, Y., Yang, S., Tian, H., & Sun, B. (2021). The research progress of organic fluorescent probe applied in food and drinking water detection. *Coordination Chemistry Reviews, 427*. https://doi.org/10.1016/j.ccr.2020.213557.

Feng, H., Liu, J., Qaitoon, A., Meng, Q., Sultanbawa, Y., Zhang, Z., ... Zhang, R. (2021). Responsive small-molecule luminescence probes for sulfite/bisulfite detection in food samples. *TrAC Trends in Analytical Chemistry, 136*, 116199. https://doi.org/10.1016/j.trac.2021.116199.

Feng, H., Meng, Q., Wang, Y., Duan, C., Wang, C., Jia, H., ... Zhang, R. (2018). Responsive fluorescence probe for selective and sensitive detection of hypochlorous acid in live cells and animals. *Chemistry – An Asian Journal, 13*(18), 2611–2618.

Gangopadhyay, A., Ali, S. S., Guria, U. N., Samanta, S. K., Sarkar, R., Datta, P., & Mahapatra, A. K. (2018). A ratiometric hypochlorite sensor guided by PET

controlled ESIPT output with real time application in commercial bleach. *New Journal of Chemistry, 42*(19), 15990–15996. https://doi.org/10.1039/C8NJ03369B.

Ge, X., Lou, Y., Su, L., Chen, B., Guo, Z., Gao, S., ... Yang, H. (2020). Single wavelength laser excitation ratiometric NIR-II fluorescent probe for molecule imaging in vivo. *Analytical Chemistry, 92*(8), 6111–6120. https://doi.org/10.1021/acs.analchem.0c00556.

Goswami, S., Das, A. K., Manna, A., Maity, A. K., Saha, P., Quah, C. K., ... Abdel-Aziz, H. A. (2014). Nanomolar detection of hypochlorite by a rhodamine-based chiral hydrazide in absolute aqueous media: Application in tap water analysis with live-cell imaging. *Analytical Chemistry, 86*(13), 6315–6322. https://doi.org/10.1021/ac500418k.

Han, J., Liu, X., Xiong, H., Wang, J., Wang, B., Song, X., & Wang, W. (2020). Investigation of the relationship between H2O2 and HClO in living cells by a bifunctional, dual-ratiometric responsive fluorescent probe. *Analytical Chemistry, 92*(7), 5134–5142. https://doi.org/10.1021/acs.analchem.9b05604.

Ikeno, T., Hanaoka, K., Iwaki, S., Myochin, T., Murayama, Y., Ohde, H., ... Urano, Y. (2019). Design and synthesis of an activatable photoacoustic probe for hypochlorous acid. *Analytical Chemistry, 91*(14), 9086–9092. https://doi.org/10.1021/acs.analchem.9b01529.

Jia, S., Wu, J., Ye, L., Zhao, F., Li, T., & Zhang, X.-X. (2019). Metagenomic assembly provides a deep insight into the antibiotic resistome alteration induced by drinking water chlorination and its correlations with bacterial host changes. *Journal of Hazardous Materials, 379*. https://doi.org/10.1016/j.jhazmat.2019.120841.

Kaushik, R., Ghosh, A., & Amilan Jose, D. (2017). Recent progress in hydrogen sulphide (H2S) sensors by metal displacement approach. *Coordination Chemistry Reviews, 347*, 141–157. https://doi.org/10.1016/j.ccr.2017.07.003.

Kwon, N., Kim, D., Swamy, K. M. K., & Yoon, J. (2021). Metal-coordinated fluorescent and luminescent probes for reactive oxygen species (ROS) and reactive nitrogen species (RNS). *Coordination Chemistry Reviews, 427*. https://doi.org/10.1016/j.ccr.2020.213581.

Li, M.-Y., Li, K., Liu, Y.-H., Zhang, H., Yu, K.-K., Liu, X., & Yu, X.-Q. (2020a). Mitochondria-immobilized fluorescent probe for the detection of hypochlorite in living cells, tissues, and zebrafishes. *Analytical Chemistry, 92*(4), 3262–3269. https://doi.org/10.1021/acs.analchem.9b05102.

Li, X., Pan, Y., Chen, H., Duan, Y., Zhou, S., Wu, W., ... Liu, B. (2020b). Specific Near-infrared probe for ultrafast imaging of lysosomal β-galactosidase in ovarian cancer cells. *Analytical Chemistry, 92*(8), 5772–5779. https://doi.org/10.1021/acs.analchem.9b05121.

Liu, Y., Sun, Y., Du, J., Lv, X., Zhao, Y., Chen, M., ... Guo, W. (2011). Highly sensitive and selective turn-on fluorescent and chromogenic probe for Cu^{2+} and ClO^{-} based on a N-picolinyl rhodamine B-hydrazide derivative. *Organic & Biomolecular Chemistry, 9*(2), 432–437. https://doi.org/10.1039/C0OB00411A.

Mocak, J., Bond, A. M., Mitchell, S., & Scollary, G. (1997). A statistical overview of standard (IUPAC and ACS) and new procedures for determining the limits of detection and quantification: Application to voltammetric and stripping techniques (Technical Report). *Pure and Applied Chemistry, 69*(2), 297–328. https://doi.org/10.1351/pac199769020297.

Ordeig, O., Mas, R., Gonzalo, J., Del Campo, F. J., Muñoz, F. J., & de Haro, C. (2005). Continuous detection of hypochlorous acid/hypochlorite for water quality monitoring and control. *Electroanalysis, 17*(18), 1641–1648. https://doi.org/10.1002/elan.200403194.

Park, J., Kim, H., Choi, Y., & Kim, Y. (2013). A ratiometric fluorescent probe based on a BODIPY–DCDHF conjugate for the detection of hypochlorous acid in living cells. *Analyst, 138*(12), 3368–3371. https://doi.org/10.1039/C3AN36820C.

Ren, H., Huo, F., & Yin, C. (2021). An ESIPT-based colorimetric and fluorescent probe with large Stokes shift for sensitive detection of hypochlorous acid and its bioimaging in cells. *New Journal of Chemistry*. https://doi.org/10.1039/D0NJ05807F.

Setsukinai, K.-I., Urano, Y., Kakinuma, K., Majima, H. J., & Nagano, T. (2003). Development of novel fluorescence probes that can reliably detect reactive oxygen species and distinguish specific species*210. *Journal of Biological Chemistry, 278*(5), 3170–3175. https://doi.org/10.1074/jbc.M209264200.

Shiraishi, Y., Yamada, C., Takagi, S., & Hirai, T. (2021). Fluorometric and colorimetric detection of hypochlorous acid and hypochlorite by a naphthalimide–dicyanoisophorone conjugate. *Journal of Photochemistry and Photobiology A: Chemistry, 406*. https://doi.org/10.1016/j.jphotochem.2020.112997.

Song, B., Wang, G., Tan, M., & Yuan, J. (2005). Synthesis and time-resolved fluorimetric application of a europium chelate-based phosphorescence probe specific for singlet oxygen. *New Journal of Chemistry, 29*(11), 1431–1438. https://doi.org/10.1039/B510611G.

Sun, Z.-N., Liu, F.-Q., Chen, Y., Tam, P. K. H., & Yang, D. (2008). A highly specific BODIPY-based fluorescent probe for the detection of hypochlorous acid. *Organic Letters, 10*(11), 2171–2174. https://doi.org/10.1021/ol800507m.

Venkatesan, P., & Wu, S.-P. (2015). A turn-on fluorescent probe for hypochlorous acid based on the oxidation of diphenyl telluride. *Analyst, 140*(4), 1349–1355. https://doi.org/10.1039/C4AN02116A.

Watanabe, T., Idehara, T., Yoshimura, Y., & Nakazawa, H. (1998). Simultaneous determination of chlorine dioxide and hypochlorite in water by high-performance liquid chromatography. *Journal of Chromatography A, 796*(2), 397–400. https://doi.org/10.1016/S0021-9673(97)01009-1.

Wu, B., Yang, J., Zhang, J., Li, Z., Li, H., & Yang, X.-F. (2019). A ratiometric fluorescent probe for the detection of endogenous hydroxyl radicals in living cells. *Talanta, 196*, 317–324. https://doi.org/10.1016/j.talanta.2018.12.065.

Wu, D., Chen, L., Xu, Q., Chen, X., & Yoon, J. (2019). Design principles, sensing mechanisms, and applications of highly specific fluorescent probes for $HOCl/OCl^{-}$. *Accounts of Chemical Research, 52*(8), 2158–2168. https://doi.org/10.1021/acs.accounts.9b00307.

Wu, L., Sedgwick, A. C., Sun, X., Bull, S. D., He, X.-P., & James, T. D. (2019). Reaction-based fluorescent probes for the detection and imaging of reactive oxygen, nitrogen, and sulfur species. *Accounts of Chemical Research, 52*(9), 2582–2597. https://doi.org/10.1021/acs.accounts.9b00302.

Wu, L., Wang, Y., Weber, M., Liu, L., Sedgwick, A. C., Bull, S. D., ... James, T. D. (2018). ESIPT-based ratiometric fluorescence probe for the intracellular imaging of peroxynitrite. *Chemical Communications, 54*(71), 9953–9956. https://doi.org/10.1039/C8CC04919J.

Wu, Y., Wang, J., Zeng, F., Huang, S., Huang, J., Xie, H., ... Wu, S. (2016). Pyrene derivative emitting red or near-infrared light with monomer/excimer conversion and its application to ratiometric detection of hypochlorite. *ACS Applied Materials & Interfaces, 8*(2), 1511–1519. https://doi.org/10.1021/acsami.5b11023.

Yadav, A., Upadhyay, Y., Bera, R. K., & Sahoo, S. K. (2020). Vitamin B6 cofactors guided highly selective fluorescent turn-on sensing of histamine using beta-cyclodextrin stabilized ZnO quantum dots. *Food Chemistry, 320*, 126611. https://doi.org/10.1016/j.foodchem.2020.126611.

Yang, D., Wang, H.-L., Sun, Z.-N., Chung, N.-W., & Shen, J.-G. (2006). A highly selective fluorescent probe for the detection and imaging of peroxynitrite in living cells. *Journal of the American Chemical Society, 128*(18), 6004–6005. https://doi.org/10.1021/ja060375610.1021/ja0603756.s001.

Zhang, R., Song, B., & Yuan, J. (2018). Bioanalytical methods for hypochlorous acid detection: Recent advances and challenges. *TrAC Trends in Analytical Chemistry, 99*, 1–33. https://doi.org/10.1016/j.trac.2017.11.015.

Zhang, R., Yong, J., Yuan, J., & Ping Xu, Z. (2020). Recent advances in the development of responsive probes for selective detection of cysteine. *Coordination Chemistry Reviews, 408*. https://doi.org/10.1016/j.ccr.2020.213182.

Zhao, N., Wu, Y.-H., Wang, R.-M., Shi, L.-X., & Chen, Z.-N. (2011). An iridium(iii) complex of oximated 2,2′-bipyridine as a sensitive phosphorescent sensor for hypochlorite. *Analyst, 136*(11), 2277–2282. https://doi.org/10.1039/C1AN15030H.

Zhu, B., Tang, W., Ren, Y., & Duan, X. (2018). Chemiluminescence of conjugated-polymer nanoparticles by direct oxidation with hypochlorite. *Analytical Chemistry, 90*(22), 13714–13722. https://doi.org/10.1021/acs.analchem.8b04109.

Zhuang, M., Ding, C., Zhu, A., & Tian, Y. (2014). Ratiometric fluorescence probe for monitoring hydroxyl radical in live cells based on gold nanoclusters. *Analytical Chemistry, 86*(3), 1829–1836. https://doi.org/10.1021/ac403810g.